Table 1 Curved beam element rotation mode eigenvalues[a]

$\Delta\phi$	Linear	Quadratic	Cubic
2	2013.	0.05688	0.00005
4	7006.	0.00234	0.00002
6	12177.	0.02387	0.00019
8	17179.	0.04258	0.00079
12	26794.	0.21930	0.00618
16	35933.	0.88204	0.02636
20	44388.	2.46182	0.08052

[a] $E = 1.0 \times 10^7$; $\nu = 0.3$; $t = 2$ in.; width = 2 in.; $I = 1.33$ in.^{4}.

Examination of the displacement function given by Eq. (1) reveals that there is one rigid body mode associated with the zeroth harmonic and two associated with the first harmonic. Eigenvalue analyses were conducted on the matrix $[L]$ for both harmonics. It was found that the representation of rigid body translation in the zeroth harmonic yielded the most critical case. For this case a plot of the internal energy versus change in angle is given in Fig. 1. The quadratic representation was obtained by setting $\beta_2 = \beta_4 = 0$. It is noted that quadratic and cubic displacement functions show a tremendous improvement over the results obtained for a linear u and v. A cubic displacement function in w was used in all three cases.

The results for a hemispherical shell undergoing large rigid body translation are shown in Fig. 2. This example confirms the eigenvalue analysis that the quadratic and cubic displacement functions are considerably better than the linear functions.

An eigenvalue analysis was also conducted on a curved beam element. A cubic function was used for the normal displacement and linear, quadratic and cubic functions were used for the meridional displacements. The results for the largest eigenvalue which should be zero for rigid body motion are shown in Table 1.

It is again noted that there is a tremendous improvement in going from a linear to a quadratic function in the meridional displacement. For both the shell and beam element the lowest elastic eigenvalue was of the order of 1.0×10^6.

In summary it has been demonstrated in this Note that implicit rigid body motion is much better represented when going from a linear to a quadratic displacement function. Static condensation makes it possible to use the higher order displacement function without increasing the size of the resulting element stiffness matrix.

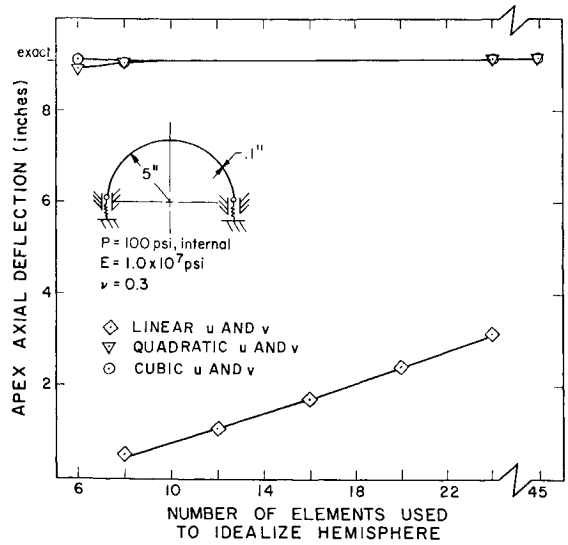

Fig. 2 Deflection analysis of a hemisphere with large rigid body motion.

References

[1] Stricklin, J. A., Navaratna, D. R., and Pian, T. H. H., "Improvements on the Analysis of Shells of Revolution by the Matrix Displacement Method," *AIAA Journal*, Vol. 4, No. 11, Nov. 1966, pp. 2069–2072.

[2] Haisler, W. E. and Stricklin, J. A., "Rigid Body Displacements of Curved Elements in the Analysis of Shells by the Matrix Displacement Method," *AIAA Journal*, Vol. 5, No. 8, Aug. 1967, pp. 1525–1527.

[3] Gallagher, R. H., "The Development and Evaluation of Matrix Methods for Thin Shell Structural Analysis," Ph.D. dissertation, 1966, State Univ. of New York at Buffalo.

[4] Schmit, L. A., Bogner, F. K., and Fox, R. L., "Finite Deflection Structural Analysis Using Plate and Shell Discrete Elements," *AIAA Journal*, Vol. 6, No. 5, May 1968, pp. 781–791.

[5] Gallagher, R. H., "Analysis of Plate and Shell Structures," *Proceedings of Application of Finite Element Methods in Civil Engineering*, Vanderbilt Univ., Nashville, Tenn., Nov. 1969, pp. 155–205.

[6] Key, S. W. and Beisinger, Z. E., "The Analysis of Thin Shells by the Finite Element Method," presented at IUTAM Symposium on High Speed Computing of Elastic Structures, Liege, Belgium, Aug. 1970.

[7] Stricklin, J. A. et al., "Nonlinear Analysis of Shells of Revolution by the Matrix Displacement Method," *AIAA Journal*, Vol. 6, No. 12, Dec. 1968, pp. 2306–2312.

[8] Stricklin, J. A. et al., "Nonlinear Dynamic Analysis of Shells of Revolution by Matrix Displacement Method," *AIAA/ASME 11th Structures, Structural Dynamics, and Materials Conference*, AIAA, New York, 1970.

[9] Witmer, E. A. et al., "An Improved Discrete-Element Analysis and Program for the Linear Elastic Static Analysis of Meridionally-Curved Variable-Thickness Branched Thin Shells of Revolution Subjected to General External Mechanical and Thermal Loads, Part I," Aeroelastic and Structures Lab. Rept. TR-146-4, March 1968, M.I.T., Cambridge, Mass.

[10] Kotanchik, J. J. "Discrete-Element Static Analysis of Bonded Double-Layer, Branched, Thin Shells of Revolution, Part 2: The SABOR V Program," Aeroelastic and Structures Lab. Rept. TR-139-6, May 1969, M.I.T., Cambridge, Mass.

Static Pressure Measurements near an Oblique Shock Wave

L. H. Back* and R. F. Cuffel†
Jet Propulsion Laboratory,
California Institute of Technology, Pasadena, Calif.

Nomenclature

d = probe diameter
l = probe length
M = Mach number
p = static pressure
p_t' = pitot pressure
p_{to} = reservoir pressure

Introduction

THIS Note is concerned with appraising readings of relatively short static pressure probes in the vicinity of an oblique shock wave. Such probes are used along with pitot tubes to determine the Mach number distribution in supersonic flowfields. In the absence of shock waves in the flow,

Received October 16, 1970. This Note presents the results of one phase of research carried out at the Jet Propulsion Laboratory, California Institute of Technology, under Contract No. NAS 7-100, sponsored by NASA.

* Member Technical Staff, Propulsion Research and Advanced Concepts Section. Associate Fellow AIAA.

† Senior Engineer, Propulsion Research and Advanced Concepts Section. Member AIAA.

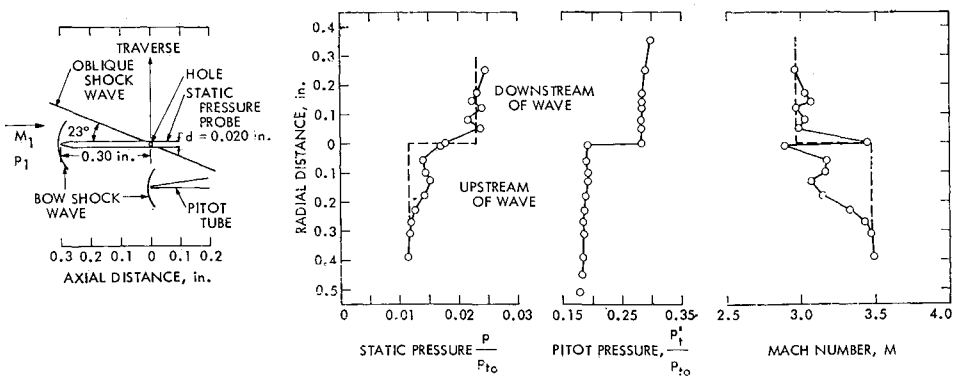

Fig. 1 Interaction measurements.

an upstream length of 15-probe diameters from the hole to the tip has been found[1] to be sufficient to allow the local static pressure upstream of the probe bow shock wave to recover within about 1%. However, when traversing the probe across an oblique shock wave, the interaction between the probe bow shock wave and the oblique shock wave can influence the flowfield along the probe, particularly where the pressure is measured. The intent of this investigation is to learn about the lateral extent of the interaction region so that measurements can be properly interpreted. There is usually no problem with obtaining accurate pitot tube measurements, because the pitot pressure is influenced by the bow shock-oblique shock wave interaction at distances less than one tip height[2]; therefore the region of influence can be reduced by using a probe with a small tip. However, the size of the static pressure probe is limited by strength considerations; in addition, the measured pressure is expected to be influenced at distances greater than a probe diameter because of the configuration of the probe and the oblique shock wave.

Measurements and Probes

The measurements were made in air flowing through an axisymmetric supersonic diffuser. The stagnation pressure upstream of the nozzle, which preceded the diffuser, was 100 psia and the stagnation temperature was 535°R. The oblique shock wave that was generated at the nozzle exit was conical at the traversing location as indicated by additional pitot tube surveys made upstream and downstream of those shown in Fig. 1. The angle between the approaching flow and the shock wave was 23°, and the Mach number upstream of the wave was about 3.5. The shock wave turned the flow through 8.3°. The axis of the conical shock was located along the centerline of the diffuser above the interaction configurations that are shown in Figs. 1 and 2; e.g., in Fig. 1 the radial distance from the centerline to the interaction was 1.17 in. Downstream of the interactions, the conical shock wave extended into a turbulent boundary layer near the wall and was subsequently reflected downstream.

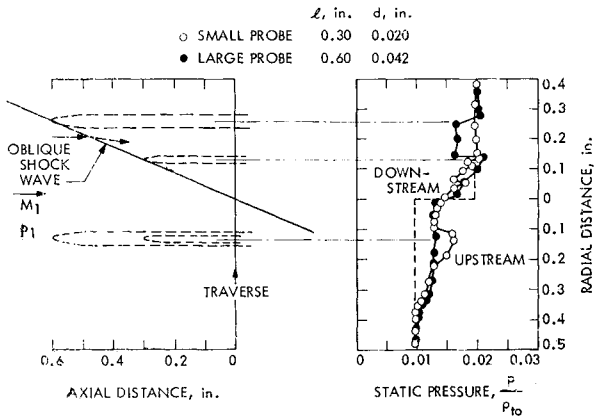

Fig. 2 Effect of probe size on static pressures readings.

Two configurations of pressure probes with blunted conical tips were used: one with an outside diameter of 0.020 in. and the other with a diameter about twice as large, 0.042 in. The smaller diameter probe had an 0.008-in. diam hole drilled on each side of the probe, and the distance from the holes to the tip was 0.30 in., or 15 diameters. The larger diameter probe which had a single 0.008-in. diam hole on its side was twice as long, 0.60 in.; so that its length in diameters 14.3 was nearly the same as that of the smaller probe. The pitot tube has a small flattened tip whose height was 0.005 in.

The probes were moved mechanically across the flow by a micrometer lead screw. The pressure difference between the motor-driven probes and a surface static pressure tap was measured with transducers and plotted continuously during the traverses. At the very slow traversing speeds used, no difference was observed in readings obtained by traversing back again in the opposite direction.

Results

Measured static and pitot pressures and calculated Mach numbers obtained from these readings are shown in Fig. 1. Below the oblique shock wave (i.e., upstream of the wave) higher static pressure readings are found than the true value. Differences between the readings and the true value arise because the flowfield along the probe in the vicinity of the hole is influenced by the probe bow shock-oblique shock wave interaction. Also the presence of the adjacent oblique shock wave can reflect incident waves that arrive from the probe back again toward the probe. The detailed nature of the shock wave interactions and ensuing wave is not known, however. Certainly the interactions themselves are more complicated than might be inferred for the case of two-intersecting shock waves of different strengths which pass through each other and are slightly bent in the process. The complexity arises from the combination of the oblique shock wave which is conical and the probe bow shock wave which is a smaller curved surface that forms an envelope around the probe. Furthermore, the pressure read by the probe is associated with a flow that varies in all directions, since a different behavior is expected above than below the probe as well as on the side where the hole is because of the shock wave configurations. The influence of this interaction seems to persist to a distance of about 0.30 in. below the oblique shock wave where the actual static pressure is apparently recovered. This distance is the same as the length of the probe and is also equivalent to 15-probe diameters. Above the oblique shock wave (i.e., downstream) the region of influence appears to be less, although a better view of this region is presented subsequently in Fig. 2.

The step increase in static pressure across the oblique shock wave shown in Fig. 1 by the dashed curve was calculated by using the oblique shock relation knowing the wave angle and upstream Mach number that was obtained from the

measured static and pitot pressures farther away from the oblique shock wave. The good correspondence between the predicted and measured pressure rise indicated, establishes confidence in the actual pressure change across the oblique shock wave and allows an appraisal of the region of probe influence. The increase in pitot pressure across the oblique shock wave is also compatible with that calculated using the oblique shock relations, e.g., experimentally $p_{t_2}'/p_{t_1}' = 1.48$, while a value of 1.50 is predicted. Of note in this connection is that the turning of the flow through an angle of 8.3° in passing through the oblique shock wave apparently did not influence the pitot tube reading downstream where the flow is inclined to the probe. The slight "blip" in the pitot pressure below the oblique shock wave is associated with a small disturbance locally in the flow rather than the presence of the oblique shock wave. This view is supported by pitot measurements at axial distances farther upstream and downstream which indicated the disturbance to lie along a streamline and thus was located at different radial distances from the oblique shock wave.

Rather large deviations in Mach number are found by using the local static and pitot pressures measured to calculate the Mach number; this occurs because of the fallacious static pressure readings. It should be mentioned that the upstream Mach number of 3.48 is not compatible with the static to total pressure ratio $p/p_{t_0} = 0.0116$ for isentropic flow up to the shock wave because the actual stagnation pressure upstream of the wave is less than the upstream reservoir pressure $p_{t_0} =$ 100 psia that is used to normalize the data. The reduction in stagnation pressure resulted from the flow passing through another oblique shock wave farther upstream.

The influence of the size of the static pressure probe on its reading is shown in Fig. 2. These measurements were made 0.5 in. downstream of those shown in Fig. 1 at a location where the static pressure was lower. The small probe is similar to that used upstream, and the larger probe is twice as long. Confidence in the actual pressure changes across the oblique shock wave is provided by the very good check with the predicted oblique shock relation shown as a dashed curve and the coincidence of both probe readings farther away from the oblique shock wave. The probes are shown at various locations to assist in the discussion of the readings.

Upstream of the oblique shock wave (Fig. 2) the larger probe readings do not have as pronounced a "hump" as observed with the small probe. Also there is a more gradual approach to the actual static pressure which is found farther away from the oblique shock wave, although this change is small for a probe that is twice as long.

Downstream of the oblique shock wave (Fig. 2) the small probe behavior is similar to that observed before in Fig. 1, although the actual static pressure does not appear to be recovered until the tip of the probe is located downstream of the oblique shock wave (a distance of 0.13 in. above the wave). The larger probe reading at this location is also in general agreement with the actual pressure. However, farther away from the oblique shock wave in the vicinity where the tip of the larger probe intersects the wave, there is a depression in the static pressure reading. The static pressure is recovered again at about 0.3 in., similar to that observed with the smaller probe when its tip was located downstream of the oblique shock wave. Apparently, once the tip of the probe is downstream of the wave, useful static pressure readings are obtained; although for longer probes meaningful readings also are found when the tip is upstream of the wave and the hole therefore is isolated downstream. Probes extending a great distance upstream would display this latter behavior too. When the probe tip is located downstream of the wave, the flow along the probe in the vicinity of the hole has originated from a location that lies above the probe (Fig. 2, flow arrows) and therefore, is apparently not influenced much by the probe bow shock-oblique shock wave interaction, and the presence of the oblique shock wave.

Summary and Conclusions

For a relatively short static pressure probe traversed across an oblique shock wave, the readings upstream of the wave were influenced by interactions at a lateral distance up to about one probe length l from the wave (15-probe diameters); although for a probe twice as long and about twice the diameter of the small probe, this lateral distance was only slightly more than $\frac{1}{2}$ the probe length. Downstream of the oblique shock wave useful static pressures were obtained once the tip of the probe was downstream of the wave (a lateral distance of about $l \tan\beta$ where β is the wave angle); although for longer probes meaningful readings are also found where the tip is upstream of the wave and the hole is isolated downstream. These trends would be the same if the wave angle β were negative rather than positive, since the results would be a mirror image of those shown. Clearly there are limitations on the use of such static pressure probes in the vicinity of shock waves; for example, in interaction studies of shock wave impingement and reflection from boundary layers.

References

[1] Cronvich, L. L., "Pressure Distributions Over a Cylinder with Conical or Hemispherical Head at Supersonic Velocities," Rept. CM-528, Feb. 1949, Applied Physics Lab, Johns Hopkins University, Silver Spring, Md.

[2] Bannink, W. J. and Nebbeling, C., "Determination of the Position of a Shock Wave from Pitot Tube Experiments," *AIAA Journal*, Vol. 7, No. 4, April 1969, pp. 796–797.

A Quantitative Measurement of Thermally Induced Stress Waves

C. M. Percival*
Sandia Laboratories, Albuquerque, N. Mex.

SINCE the paper by Danilovskaya[1] in 1950 many authors have considered the theory of the dynamic behavior of elastic materials upon exposure to very rapid heating such as can occur on exposure to electromagnetic radiation of various kinds. When the energy deposition time is of the same order as the mechanical response time of the material, dynamic stresses can develop. These stresses are a result of the material's inertial resistance to rapid thermal expansion. This author, in a previous paper,[2] addressed the problem of thermally generated stress waves in a one-dimensional stress field, the finite rod problem. This paper reported the first measurements of elastic stress waves generated in a solid bar due to in-depth absorption of laser radiation. Papers by Morland[3] and Bushnell and McCloskey[4] dealt with the similar problem in one-dimensional strain. Although the theory presented in these papers is valid, measurements of thermally generated stress waves in good quantitative agreement with the one-dimensional strain theory have not as yet been reported.

This Note will describe such a quantitative measurement of laser generated stress waves in which both the wave shape and amplitude agree with the theoretical predictions. The deposition time and the energy penetration depth in the material are such that the effect of a finite deposition time must be considered.

Experiment

The energy source used in the experiment was a Q-switched ruby laser. The maximum output of the laser was 8 joules in

Received October 26, 1970.
Work supported by U.S. Atomic Energy Commission.
* Staff Member, Composites Research and Development Department.